Research Article | Vol. 25, No. 22 | 30 Oct 2017 | OPTICS EXPRESS 27706
Optics EXPRESS

2.5 TW, two-cycle IR laser pulses via frequency domain optical parametric amplification

V. Gruson,[1,2,*] G. Ernotte,[1] P. Lassonde,[1] A. Laramée,[1] M. R. Bionta,[1] M. Chaker,[1] L. Di Mauro,[2] P. B. Corkum,[3] H. Ibrahim,[1] B. E. Schmidt,[4] and F. Légaré[1]

[1]*Centre Énergie Matériaux et Télécommunications, Institut National de la Recherche Scientifique, 1650 Boulevard Lionel-Boulet, Varennes, Québec, J3X1S2, Canada*
[2]*Department of Physics, The Ohio State University, Columbus, Ohio 43210, USA*
[3]*Joint Attosecond Science Laboratory, University of Ottawa and National Research Council of Canada, 100 Sussex Dr, Ottawa K1N 5A2, Canada*
[4]*few-cycle, Inc., 2890 rue de Beaurivage, Montréal, Québec H1L5W5, Canada*
[*]*vincent.gruson@emt.inrs.ca*

Abstract: Broadband optical parametric amplification in the IR region has reached a new milestone through the use of a non-collinear Frequency domain Optical Parametric Amplification system. We report a laser source delivering 11.6 fs pulses with 30 mJ of energy at a central wavelength of 1.8 μm at 10 Hz repetition rate corresponding to a peak power of 2.5 TW. The peak power scaling is accompanied by a pulse shortening of about 20% upon amplification due to the spectral reshaping with higher gain in the spectral wings. This source paves the way for high flux soft X-ray pulses and IR-driven laser wakefield acceleration.

OCIS codes: (320.0320) Ultrafast optics; (320.5540) Pulse shaping; (320.7110) Ultrafast nonlinear optics (020.2649) Strong field laser physics.

References and links

1. P. B. Corkum, "Plasma perspective on strong-field multiphoton ionization," Phys. Rev. Lett. **71**, 1994 (1993).
2. T. Popmintchev, M.-C. Chen, D. Popmintchev, P. Arpin, S. Brown, S. Ališauskas, G. Andriukaitis, T. Balčiunas, O. D. Mücke, A. Pugzlys, A. Baltuška, B. Shim, S. E. Schrauth, A. Gaeta, C. Hernández-García, L. Plaja, A. Becker, A. Jaron-Becker, M. M. Murnane, and H. C. Kapteyn, "Bright coherent ultrahigh harmonics in the kev x-ray regime from mid-infrared femtosecond lasers," Science **336**, 1287–1291 (2012).
3. M. Clerici, M. Peccianti, B. E. Schmidt, L. Caspani, M. Shalaby, M. Giguère, A. Lotti, A. Couairon, F. Légaré, T. Ozaki, D. Faccio, and R. Morandotti, "Wavelength scaling of terahertz generation by gas ionization," Phys. Rev. Lett. **110**, 253901 (2013).
4. S. Payeur, S. Fourmaux, B. E. Schmidt, J. P. MacLean, C. Tchervenkov, F. Légaré, M. Piché, and J. C. Kieffer, "Generation of a beam of fast electrons by tightly focusing a radially polarized ultrashort laser pulse," Appl. Phys. Lett. **101**, 041105 (2012).
5. T. Tajima and J. M. Dawson, "Laser electron accelerator," Phys. Rev. Lett. **43**, 267–270 (1979).
6. S. Akhmanov, A. Kovrigin, A. Piskarskas, V. Fadeev, and R. Khokhlov, "Observation of parametric amplification in the optical range," Jetp. Lett. **2**, 191 (1965).
7. C. Vozzi, F. Calegari, E. Benedetti, S. Gasilov, G. Sansone, G. Cerullo, M. Nisoli, S. D. Silvestri, and S. Stagira, "Millijoule-level phase-stabilized few-optical-cycle infrared parametric source," Opt. Lett. **32**, 2957–2959 (2007).
8. N. Thiré, S. Beaulieu, V. Cardin, A. Laramée, V. Wanie, B. E. Schmidt, and F. Légaré, "10 mJ 5-cycle pulses at 1.8 μm through optical parametric amplification," Appl. Phys. Lett. **106**, 091110 (2015).
9. D. Strickland and G. Mourou, "Compression of amplified chirped optical pulses," Opt. Commun. **56**, 219 (1985).
10. A. Dubietis, G. Jonušauskas, and A. Piskarskas, "Powerful femtosecond pulse generation by chirped and stretched pulse parametric amplification in BBO crystal," Opt. Commun. **88**, 437–440 (1992).
11. S. Witte and K. S. Eikema, "Ultrafast optical parametric chirped-pulse amplification," IEEE J. Sel. Top. Quantum Electron. **18**, 296–307 (2012).
12. G. Andriukaitis, T. Balčiūnas, S. Ališauskas, A. Pugžlys, A. Baltuška, T. Popmintchev, M.-C. Chen, M. M. Murnane, and H. C. Kapteyn, "90 GW peak power few-cycle mid-infrared pulses from an optical parametric amplifier," Opt. Lett. **36**, 2755–2757 (2011).
13. D. Herrmann, L. Veisz, R. Tautz, F. Tavella, K. Schmid, V. Pervak, and F. Krausz, "Generation of sub-three-cycle, 16 TW light pulses by using noncollinear optical parametric chirped-pulse amplification," Opt. Lett. **34**, 2459–2461 (2009).

#305625 https://doi.org/10.1364/OE.25.027706
Journal © 2017 Received 25 Aug 2017; revised 5 Oct 2017; accepted 6 Oct 2017; published 25 Oct 2017

Optics EXPRESS

14. N. Ishii, K. Kaneshima, K. Kitano, T. Kanai, S. Watanabe, and J. Itatani, "Sub-two-cycle, carrier-envelope phase-stable, intense optical pulses at 1.6 μm from a BiB_3o_6 optical parametric chirped-pulse amplifier," Opt. Lett. **37**, 4182–4184 (2012).
15. Y. Yin, J. Li, X. Ren, K. Zhao, Y. Wu, E. Cunningham, and Z. Chang, "High-efficiency optical parametric chirped-pulse amplifier in BiB_3o_6 for generation of 3 mJ, two-cycle, carrier-envelope-phase-stable pulses at 1.7 μm," Opt. Lett. **41**, 1142–1145 (2016).
16. Y. Yin, J. Li, X. Ren, Y. Wang, A. Chew, and Z. Chang, "High-energy two-cycle pulses at 3.2 μm by a broadband-pumped dual-chirped optical parametric amplification," Opt. Express **24**, 24989–24998 (2016).
17. A. Harth, M. Schultze, T. Lang, T. Binhammer, S. Rausch, and U. Morgner, "Two-color pumped OPCPA system emitting spectra spanning 1.5 octaves from VIS to NIR," Opt. Express **20**, 3076–3081 (2012).
18. Y. Fu, E. J. Takahashi, B. Xue, and K. Midorikawa, "Generation of a 200-mJ class infrared femtosecond laser by dual-chirped optical parametric amplification," in "Conference on Lasers and Electro-Optics" (Optical Society of America, 2017), p. SM3I.3.
19. B. E. Schmidt, N. Thiré, M. Boivin, A. Laramée, F. Poitras, G. Lebrun, T. Ozaki, H. Ibrahim, and F. Légaré, "Frequency domain optical parametric amplification," Nature Communications **5** (2014).
20. B. E. Schmidt, P. Lassonde, G. Ernotte, M. Clerici, R. Morandotti, H. Ibrahim and F. Légaré, "Decoupling Frequencies, Amplitudes and Phases in Nonlinear Optics," Sci. Rep. **7**, 7861 (2017).
21. C. Froehly, "Optical processing of picosecond laser pulses," J. Opt. **12**, 25 (1981).
22. P. Lassonde, N. Thiré, L. Arissian, G. Ernotte, F. Poitras, T. Ozaki, A. Larameé, M. Boivin, H. Ibrahim, F. Légaré, "High gain Frequency domain Optical Parametric Amplification," IEEE J. Sel. Top. Quantum Electron. **21**, 1–10 (2015).
23. C. R. Phillips, B. W. Mayer, L. Gallmann and U. Keller, "Frequency-domain nonlinear optics in two-dimensionally patterned quasi-phase-matching media," Opt. Express **14**, 15940–15953 (2016).
24. M. Nisoli, S. De Silvestri, and O. Svelto, "Generation of high energy 10 fs pulses by a new pulse compression technique," Appl. Phys. Lett. **68**, 2793–2795 (1996).
25. B. E. Schmidt, P. Béjot, M. Giguère, A. D. Shiner, C. Trallero-Herrero, E. Bisson, J. Kasparian, J.-P. Wolf, D. M. Villeneuve, J.-C. Kieffer, P. B. Corkum, and F. Légaré, "Compression of 1.8 μm laser pulses to sub two optical cycles with bulk material," Appl. Phys. Lett. **96**, 121109 (2010).
26. V. Cardin, N. Thiré, S. Beaulieu, V. Wanie, F. Légaré, and B. E. Schmidt, "0.42 TW 2-cycle pulses at 1.8 μm via hollow-core fiber compression," Appl. Phys. Lett. **107**, 181101 (2015).
27. D. J. Kane, "Recent progress toward real-time measurement of ultrashort laser pulses," IEEE J. Quantum Electron **35**, 421–431 (1999).
28. D. Wang, Y. Leng, and Z. Xu, "Measurement of nonlinear refractive index coefficient of inert gases with hollow-core fiber," Appl. Phys. B **111**, 447–452 (2013).
29. C. Baumgarten, M. Pedicone, H. Bravo, H. Wang, L. Yin, C. S. Menoni, J. J. Rocca, and B. A. Reagan, "1 J, 0.5 kHz repetition rate picosecond laser," Opt. Lett. **41**, 3339–3342 (2016).
30. G. Fan, T. Balčiūnas, T. Kanai, T. Flöry, G. Andriukaitis, B. E. Schmidt, F. Légaré, and A. Baltuška, "Hollow-core-waveguide compression of multi-millijoule cep-stable 3.2 μm pulses," Optica **3**, 1308–1311 (2016).
31. X. C. Zhang, A. Shkurinov, and Y. Zhang, "Extreme terahertz science," Nat. Photonics **11**, 16–18 (2017).

1. Introduction

For the past decade, tremendous efforts have been put towards the development of intense, ultrashort laser sources in the infrared spectral range. This region is of great interest for strong field laser physics as the ponderomotive energy ($U_p = I\lambda^2$) is proportional to the laser intensity I and scales quadratically with the laser wavelength λ [1]. One important application is the scaling of high harmonic generation to the keV photon energy range [2]. In the case of THz generation, it has been shown [3] that the THz flux increases with the wavelength as $\sim \lambda^5$. Finally, direct electron acceleration [4], together with laser wakefield electron acceleration [5] are also strong field phenomena that benefit from scaling the ponderomotive energy.

To generate wavelength tunable, high intensity IR pulses, Optical Parametric Amplification (OPA, [6]) has been the principal approach. It is based on a nonlinear interaction involving virtual states, which does not limit the gain bandwidth by electronic transitions. For an efficient OPA process one must ensure good phase-matching, as described by $\Delta k = k_p - k_s - k_i$, where $k(\omega) = n(\omega)\omega/c$ corresponds to the linear momentum of the photon in the nonlinear medium; n is the refractive index, ω is the photon angular frequency, c is the speed of light and where p, s and i refers to the pump, signal and idler beam respectively. This amplification scheme opened the way towards high peak power IR laser sources [7, 8]. Despite that, when considering broadband

Optics EXPRESS

spectra supporting few-cycle pulses, the scheme suffers from gain narrowing problems, as it is difficult to comply with the phase-matching condition over a broad spectral bandwidth. Group velocity mismatch (GVM) must also be taken into account, as the velocities of the different pulses (p,s,i) propagating through the nonlinear medium depend on the refractive index, which causes a loss of temporal overlap. To enable few-cycles pulses with multi-mJ amplification, the Chirped Pulse Amplification (CPA) [9] and OPA techniques have been combined, leading to the Optical Parametric Chirped Pulse Amplification scheme (OPCPA, [10, 11]). This method enables high-power amplification on the multi-mJ level [12], even for pulses shorter than three-cycles [13–15]. The pulses have to be stretched to the picosecond time duration and are then amplified using a pump of similar duration. This technique was extended to other amplification schemes, such as Dual-Chirped OPA [16] or two-color pumping [17]. However, all those conventional time domain schemes discussed above are facing similar issues, like gain narrowing due to time dependent gain function associated to the pump temporal shape (typically Gaussian), or the energy restricted scalability due to limited sizes of nonlinear crystals, associated to damage threshold. IR OPAs have been limited to the sub-TW peak power level, until recently where Y. Fu, E. J. Takahashi, B. Xue, and K. Midorikawa, [18] presented a 2 TW level multicycle laser source with 40fs duration.

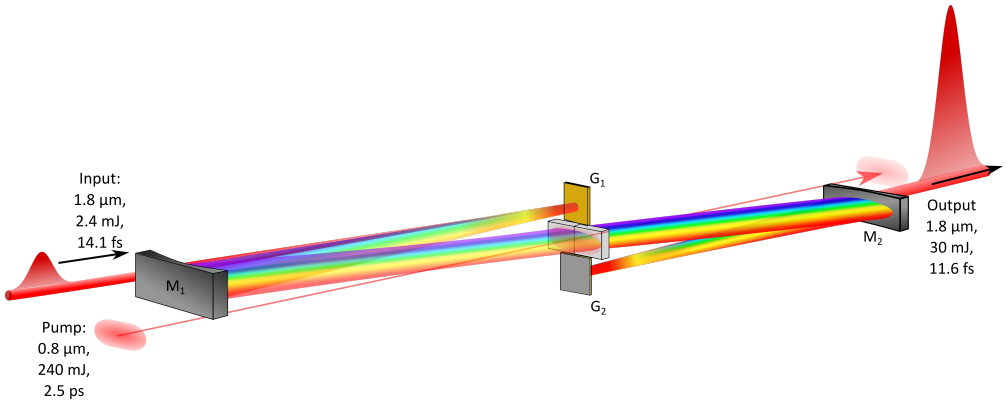

Fig. 1. A 14.1 fs, 2.4 mJ, 1.8 μm source is injected into a 4f setup, composed of two gratings G1 and G2, and two cylindrical mirrors M1 and M2. Two BBO crystals (22x15x6 mm each) are installed in the Fourier Plane, enabling amplification up to 30 mJ with an output pulse duration of 11.6 fs, using an 800 nm, 240 mJ, 2.5 ps pump source.

Here, we demonstrate for the first time multi-TW peak power at 1.8 μm, by amplifying two-cycle pulses up to 30 mJ according to a Frequency Domain Optical Parametric Amplification (FOPA, [19]) scheme. This IR peak power of 2.5 TW is reached by amplifying 2.4 mJ seed pulses with a 240 mJ Ti:Sapphire (Ti-Sa) pump laser.

Being a specific application of Fourier nonlinear optics [20], The idea behind FOPA is to amplify few-cycle pulses in the frequency domain instead of the time domain like OPCPA. This is achieved using a 4f setup as displayed Fig. 1. The spectral components of a collimated input pulse are angularly dispersed using grating G1. A collimating mirror M1 is placed at the focal distance f from the grating, enabling the collimation of the spectral components. Each of the reflected

Optics EXPRESS

spectral components is focused into a separate focus with all foci aligned in the Fourier Plane (FP). To this point, the pulses have undergone a first, (continuous) optical Fourier transformation from the time to the frequency domain. A symmetric setup following the FP performs a second Fourier transformation and recovers the original beam in time domain. Such an arrangement in combination with mode-locked lasers was first introduced in 1981 for ps pulse shaping [21]. Pulse shaping is generally achieved by applying an amplitude and/or phase modulation in the FP. In the case of FOPA, a gain function is introduced in the FP where narrowband spectral slices can be amplified independently, using a mosaic of crystals installed in parallel. The proof-of-principle has been demonstrated through the amplification of two-cycle pulses at 1.8 μm pulses from 0.2 to 1.4 mJ, using a set of 4 beta-barium borate (BBO), crystals with a pump energy of 13 mJ at 800 nm [19]. Following this demonstration, P. Lassonde and colleagues showed that the FOPA can also be used as a high gain amplification unit, where they demonstrate a gain of roughly 2000, from 1 nJ to 2 μJ at 800 nm, using 150 μJ of pump at 400 nm [22]. Finally, the group of U. Keller [23] extended the FOPA concept to the mid-IR spectral region, by amplifying a 3.4 μm source, using a 2D quasi-phase-matched medium.

2. Experimental setup

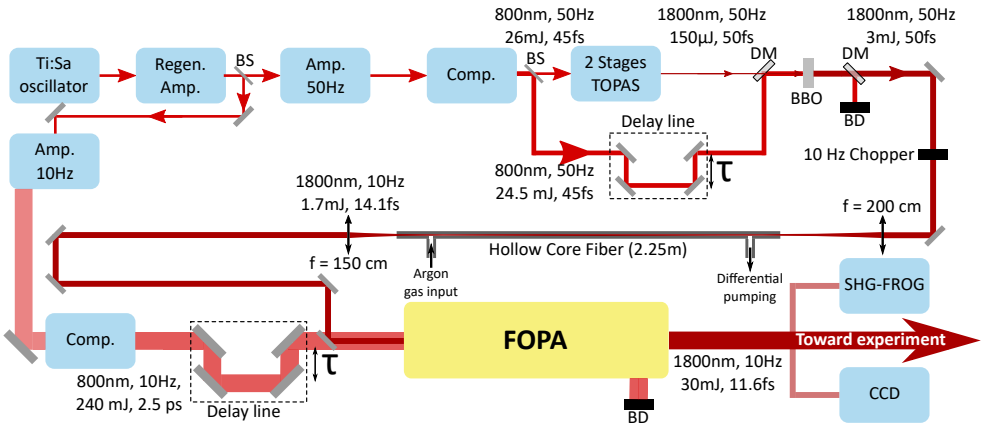

Fig. 2. Experimental setup as described in the text. Amp: Amplifier, BS : Beam Splitter, Comp. : Compressor, DM : Dichroic Mirror, BD : Beam Dump.

Two synchronized Ti-Sa lasers sources of the Advanced Laser Light Source (ALLS) are used (see Fig. 2). An 800 nm, 240 mJ, 10 Hz source with vertical polarization is used to pump the FOPA, while the 26 mJ, 800 nm central wavelength, 45 fs FWHM pulse duration, 50 Hz beamline is used to generate the seed pulses at 1.8 μm. The two sources originate from the same oscillator. To generate the seed pulses, first, 1.1 mJ, 800 nm pulses (50 Hz) are coupled to a two stages commercial TOPAS system (Light Conversion), producing 150 μJ of 1.8 μm. The output of the TOPAS is spatially filtered to ensure a clean and defined mode which is preserved in the subsequent amplification process. The last stage is a homemade high energy OPA [8], where the seed is pumped by 25 mJ of 800 nm in a 20x20x1.5 mm Type-I BBO crystal (θ = 19.9°). From this stage, a 1.8 μm pulse with 4 mJ and 50 fs FWHM duration is obtained. The seed passes through a chopper to reduce its repetition rate to 10 Hz. The beam is then focused into a stretched hollow-core fiber (HCF), for spectral broadening followed by dispersion compensation using linear propagation in fused silica [24–26]. For this, an f=2 m long focus lens is used, giving a $1/e^2$ focal spot size close to 750 μm. The fiber itself is 2.2 m long with a 1 mm inner core

Optics EXPRESS

diameter. This system is installed under vaccuum and a pressure gradient is applied with 2 bar backing pressure of Argon at the output of the fiber. Argon gas is chosen due to its high nonlinear index ($n_2 = 6.7x10^{20}\ cm^2/W$, [28]) and low cost. The transmission through this setup is $\sim 60\%$, corresponding to 2.4 mJ output energy within a spectral bandwidth from 1400 to 2200 nm. By adding a 2.5 mm thick fused silica plate, the pulses are compressed down to two-cycle duration with a horizontal polarization. At the fiber output, a collimating 1.5 m lens is installed, providing a 7.5 mm FWHM diameter. The collimated beam is then amplified in the FOPA.

For the high energy FOPA presented here, several modifications have been applied compared to previous versions. First, cylindrical mirrors were introduced instead of spherical ones to match the increased seed beam size to the pump beam in the FP. Second, the maximum interaction region has been increased up to 44x15 mm using only two type-I BBO crystals (22x15 mm each). This allows for a significant spatial extension of the pump beam, opening the door to high-energy amplification without reaching the material's damage threshold. Third, a non-collinear geometry between the seed and pump beams has been implemented, establishing a way to spatially separate the amplified from the pump beam at the FOPA output. The 1.8 μm source is angularly dispersed in the horizontal plane with a 53 l/mm grating (Richardson Grating) close to Littrow configuration ($\theta_{in} = \theta_{out} = 2.7°$), enabling the separation of the different spectral components with maximum reflectivity. The beam is then focused using a f = 600 mm cylindrical mirror, focusing in the horizontal direction, while maintaining the vertical dimension. This mirror is slightly tilted so that the output beam has a vertical angle of 1.2°. From this combination, the seed dimensions are 7.5x30 mm in the Fourier plane, with a 2.33 ps FWHM pulse duration. The seed duration in the FP has been characterized in the following way: we measured the energy of the amplified source compared to the seed-pump delay. To do so, the pump was reduced to 10% of its maximum energy (24 mJ), while its duration was reduced to 50 fs. As the seed pulse duration in the FP is expected to be on the picosecond timescale, using a fs pump enables the full temporal characterization of the seed in the FP. Results are displayed Fig. 3(a). Using a Gaussian fit, one retrieves a FWHM of 2.33 ps.

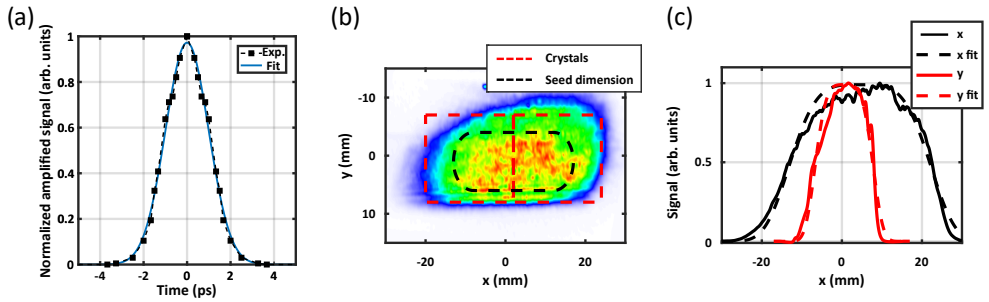

Fig. 3. (a) Measured seed pulse duration in the Fourier plane. (b) Pump beam profile at the Fourier plane. The red rectangles correspond to the crystals position in the FP, the black curve to the seed dimension in the FP. (c) Integrated pump beam profile (plain lines) and fit (dashed lines) in the horizontal (x, black) and vertical (y, red) dimension. The fit results give a FWHM of 35 mm in the x dimension and 14.8 mm in the y dimension.

An analytical formula giving the seed pulse duration is available in [22] and is displayed in Equation 1, where λ_c is the central wavelength, d_{in} is the input beam diameter at FWHM intensity, g is the grating groove separation and c is the speed of light.

Optics EXPRESS

$$\Delta t_{FP} = \frac{\lambda_c d_{in}}{gc}\left[1 - \left(\frac{\lambda_c}{2g}\right)^2\right]^{-1/2} \quad (1)$$

Taking our experimental values (λ_c=1800nm, d_{in}=7.5mm, g=19 μm), one gets Δt_{FP}=2.4 ps, being in good agreement with the experimental value.

For the amplification, two Type-1 BBO crystals (United Crystals, 22x15 mm aperture and 6 mm width) are used, with a phase-matching angle of $\theta = 24.6°$ for both crystals. Fine-tuning of the phase-matching for each crystal is achieved using two homemade goniometers with micrometric precision. An identical mirror and grating are used to recombine the amplified beam.

To obtain a homogeneous amplification over the entire spectral bandwidth, we tailor the spatial shape of the pump such that it matches that of the seed. To do so, a diffractive optical element is installed in the pump beam of the TiSa Laser. This homogenizes the TiSa output to provide a round, flat top beam. The beam then propagates through the compressor, adjusted such that the pulse duration matches the seed pulse duration, *i.e*. 2.4 ps. At the compressor output, a translation stage is used to temporally overlap the pump and seed pulses in the FP. To finalize the pump shaping, the beam is sent into a cylindrical afocal system (F3 = 680mm and F4 = -450 mm). This leads to a rectangular shaped hyper Gaussian pump beam, with 35x15 mm^2 dimension. The pump near field profile in the FP is displayed in Fig. 3(b). To illustrate the matching of the pump and the seed beams, we draw in red the position of the two BBO crystals used for amplification together with a sketch of the seed shape (in black) in the FP. The two dimensions of the pump near field profile are being integrated and fitted with a hyper Gaussian profile:

$$F(x) = A + Be^{\left(\frac{(x-x_0)}{2\sigma_x}\right)^{2N}} \quad (2)$$

with A the offset, B the amplitude, x_0 the origin, σ_x the width at $1/e^2$ and N being the hyper Gaussian order. From this, we get σ_x = 35 mm and σ_y = 14.8 mm, with N = 2, which is bigger than the seed dimension. Moreover, the central part of the pump spatial profile is almost flat, meaning that the amplification is homogeneous.

At the FOPA exit, several characterization devices are installed: a Flea2 CCD (PointGrey) to characterize the far-field profile at the focus of a f=600 mm lens, and a homemade SHG-FROG.

3. Results

The HE-FOPA output energy scaling versus pump energy is displayed in Fig. 4, as well as the conversion efficiency, defined as the ratio between the final amplified output energy over the input pump energy incident in the FP. A maximum energy of 30 mJ is extracted after the FOPA when pumping with 240 mJ. The scaling is linear with the pump energy over this range of pump energies. This linear evolution means that the conversion efficiency is close to constant, with a mean value of 13.5% after the FOPA. Since the output grating has a reflectivity $R \approx 75\%$, the conversion efficiency right after amplification in the FP is actually higher, around 18%.

We also display the far-field profiles of the seed before the FOPA, after the FOPA and of the amplified beam Fig. 4. These images are obtained through two-photon absorption on a standard CCD camera. We observe that there is no noticeable difference between the three profiles, as well as the beam size, meaning that the spatial properties are conserved. Also, no spatial chirp can be discerned.

Next, we characterize the spectral properties. Four spectra are displayed in Fig. 5(a), corresponding to the magnified (by 10.7) seed spectra (blue) and three amplified spectra obtained with 80 (yellow), 165 (green) and 240 (red) mJ of pump energy, respectively . The two crystals junction is displayed with a vertical, dashed, black line. The broadband seed spectrum extends from the [1450-2200] nm range. We now consider the amplified spectra. The whole spectra are amplified

Optics EXPRESS

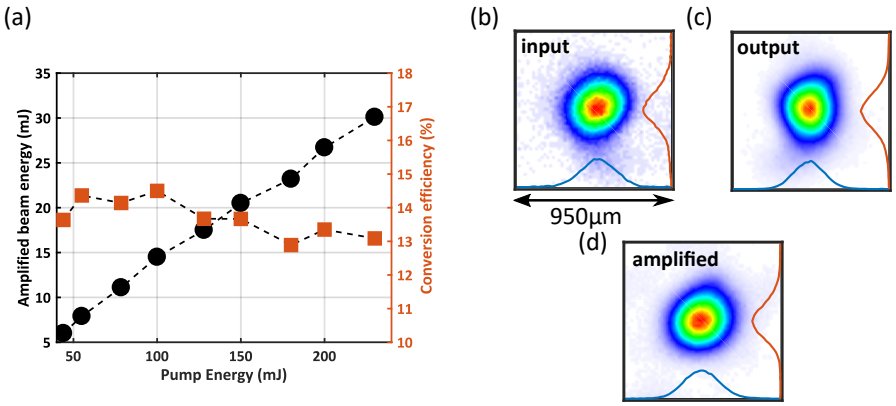

Fig. 4. (a) The amplified beam energy is plotted (black curve) as a function of the pump energy, as well as the conversion efficiency (red), defined as the ratio between the amplified output energy subsequent to the FOPA and the pump energy in the Fourier plane. (b-d) Three far-field profiles are displayed, (b) the input seed, (c) the output seed without amplification and (d) the amplified beam profile at 2.4 TW of peak power.

without saturation effects, even when pumped with 240 mJ. We note that higher gain is observed on the spectral wings. We calculate the spectral gain, defined as the ratio between the amplified spectral intensity over the seed spectral intensity, to quantitatively assess the total amplification as displayed in Fig. 5(b). A spectral gain of around 13 is achieved for the most intense part of the seed spectrum ([1600-2000] nm range), while a gain of over 30 is reached for the blue edge of the spectra ([1450-1550] nm) and over 40 for the [2100-2200] nm range with a peak at 90 around 2170 nm. From this, several points need to be addressed. The red part of the spectra shows a higher gain than the blue side; however, the gain function is slightly less homogeneous on the red side (with increasing amplification the maximum around 2000 nm is more and more pronounced). In addition, we notice from the spectral gain curve, that the amplified spectra can be shaped, leading to a gain broadening, as opposed to the typical gain narrowing effect encountered in standard amplification processes (OPA, OPCPA). This means that in addition to amplification, one can also shape/shorten the pulse. We observe from the spectra presented in Fig. 5(a) that the amplified spectra tend towards a flat-top shape, leading to a sinc function in time domain. The steeper edge on the red side of the spectrum stems from the edge of the pump beam. The gain broadening effect can be adjusted by modifying the phase-matching of our nonlinear crystal, through the use of more crystals in the FP, or by spatially tailoring the pump. In the case of Fig. 5(a), the pump was spatially larger than the seed, providing a homogeneous energy distribution.

Finally, we show in Fig. 5 (c) the SHG-FROG trace of the seed after compression in a high energy hollow-core fiber [26] and (d), the SHG-FROG trace of the amplified beam. Under each SHG-FROG, the retrieved intensity and phase is plotted, using a standard PCGPA algorithm [27]. From this reconstruction, we obtained a pulse duration of 14.1 fs FWHM after compression. Remarkably, the amplified output duration is reduced by about 20%, down to 11.6 fs. We explain this rather unusual amplifier behavior by the enhanced spectral gain in the wings of the spectrum. It raises the power spectral density of seed components from the lower percent level to more than 5% such that they efficiently contribute to the central peak of the temporal envelope. We note, that this pulse shortening does not represent a nonlinear compression step. It requires the presence of weak spectral components with a suitable spectral phase. In a conventional time domain scheme like OPCPA, however, it is very unlikely that such low spectral seed components

Optics EXPRESS

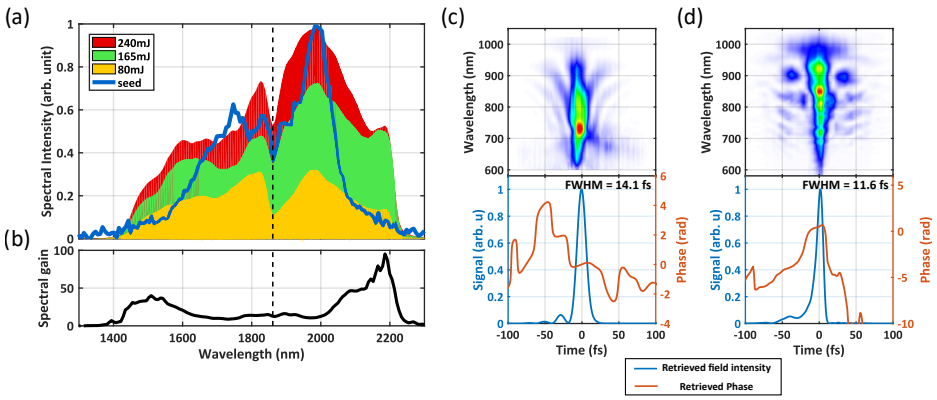

Fig. 5. (a) Magnified seed spectra (factor of 10.7) with three amplified spectra, obtained with 80, 165 and 240 mJ of pump energy, respectively. (b) Spectral gain, defined as the ratio of the amplified spectral intensity over the seed spectral intensity. In both figures, a vertical, dashed, black line is displayed, showing the junction wavelength of the two crystals. (c) Experimental SHG-FROG trace of the pulses after the fiber and retrieved intensity (blue) and phase (red), leading to a FWHM duration of 14.1 fs. (d) Experimental SHG-FROG trace of the amplified pulses and retrieved intensity (blue) and phase (red), leading to a FWHM duration of 11.6 fs.

would experience the same temporal boost as seen in the FOPA. The autocorrelation of the compressed seed pulse (not displayed) exhibits a small pedestal, around 13% of the maximum field intensity. The general shape of the seed pulse is maintained during the amplification process. Also the small pedestal of about 17% of the maximum heights has been present in the seed pulse at similar heights.

4. Conclusion

To conclude, a new generation of FOPA has enabled the development of a high peak-power source delivering two-cycle pulses with 30 mJ of energy at 10 Hz repetition rate, corresponding to 2.5 TW peak power. On the short term, our goal is to extend this performance to the 10 TW level using Joule-level Ti-Sa pump pulses. Such peak power can nowadays also be achieved with high average power, through the use of recently developed cryogenically cooled Yb:YAG lasers delivering 1 J per pulse at 500 Hz within 5 ps duration [29]. This unique technology will be ideal to push the FOPA technology up to the IR spectral range. One could imagine amplifying few-cycle 3.2 μm pulses obtained from hollow core fiber compression [30]. Those multi-TW IR few-cycle pulses are now within reach and will be ideal for developing a rainbow of high flux secondary sources, from the THz to the hard X-ray spectral range, combined with ultrashort electron bunches. Among many applications, such a spectral range will be unique to image and control ultrafast processes in the condensed matter [31].

Funding

Natural Sciences and Engineering Research Council of Canada (NSERC); Fonds de Recherche du Québec - Nature et Technologies (FRQNT); MESI; Canada Foundation for Innovation (CFI-MSI); Defense Advanced Research Projects Agency (DARPA) PULSE Program; Air Force Office of Scientific Research (AFOSR) under MURI, Award No. FA9550-16-1-0013

Optics EXPRESS

Acknowledgments

We thank Carol Morissette for his technical contribution.